Colloid-Facilitated Transport of Cesium in Variably Saturated Hanford Sediments

ARTICLE *in* ENVIRONMENTAL SCIENCE AND TECHNOLOGY · JUNE 2005

Impact Factor: 5.33 · DOI: 10.1021/es048978+ · Source: PubMed

4 AUTHORS, INCLUDING:

James B Harsh
Washington State University
90 PUBLICATIONS **1,709** CITATIONS
SEE PROFILE

Peter C Lichtner
Los Alamos National Laboratory
75 PUBLICATIONS **1,939** CITATIONS
SEE PROFILE

Environ. Sci. Technol. **2005**, *39,* 3435−3442

Colloid-Facilitated Transport of Cesium in Variably Saturated Hanford Sediments

GANG CHEN, MARKUS FLURY,* AND JAMES B. HARSH

Department of Crop and Soil Sciences, Center for Multiphase Environmental Research, Washington State University, Pullman, Washington 99164-6420

PETER C. LICHTNER

Earth and Environmental Sciences, Los Alamos National Laboratory, Los Alamos, New Mexico 87545

Radioactive ^{137}Cs has leaked from underground waste tanks into the vadose zone at the Hanford Reservation in south-central Washington State. There is concern that ^{137}Cs, currently located in the vadose zone, can reach the groundwater. In this study, we investigated whether, and to what extent, colloidal particles can facilitate the transport of ^{137}Cs at Hanford. We used colloidal materials isolated from Hanford sediments. Transport experiments were conducted under variably saturated, steady-state flow conditions in repacked, 20 cm long Hanford sediment columns, with effective water saturations ranging from 0.2 to 1.0. Cesium, pre-associated with colloids, was stripped off during transport through the sediments. The higher the flow rates, the less Cs was stripped off, indicating in part that Cs desorption from carrying colloids was a residence-time-dependent process. Depending on the flow rate, up to 70% of the initially sorbed Cs desorbed from colloidal carriers and was captured in the stationary sediments. Less Cs was stripped off colloids under unsaturated than under saturated flow conditions at similar flow rates. This phenomenon was likely due to the reduced availability of sorption sites for Cs on the sediments as the water content decreased and water flow was divided between mobile and immobile regions.

Introduction

Colloid-facilitated transport of radionuclides in porous media has been inferred from various field (*1, 2*) and laboratory experiments (*3*−*5*). Radionuclides susceptible to colloid-facilitated transport are strongly sorbing elements such as Cs, Pu, and Am. As ^{137}Cs constitutes a major portion of the radioactive inventory at the U.S. Department of Energy's (DOE) nuclear facilities, it is important to understand the environmental fate and transport of this radionuclide.

From laboratory experiments, we have evidence that Cs movement can be enhanced by amorphous silica (*5*) and crystalline aluminosilicate colloids (*4, 6*). The extent of the enhancement depends on the porous medium's particle size distribution (*5*), the colloid concentration, and the solution ionic strength (*4, 6*). In most laboratory experiments, the porous matrix consisted of glass beads and silica sand, which have a low sorption affinity for Cs. In natural porous media, however, the stationary solid phase can effectively compete with colloids for Cs sorption (*7*). Cs sorption is an ion exchange process and, therefore, is controlled by the relative sorption affinity of colloids and the stationary phase.

Cesium attaches to colloids usually via ion-exchange. Consequently, Cs can adsorb to colloidal particles in contaminated subsurface regions but may desorb when Cs-containing colloids move through a yet uncontaminated zone (*8*). If the porous medium has a high sorption affinity for Cs, Cs may be effectively stripped off the colloidal carrier (*7*). Such desorption from colloids and adsorption to the stationary solid phase will counteract the colloid-facilitated movement of Cs. On the other hand, if Cs adsorption occurs within the interlayer of colloidal illite, Cs may not easily desorb from carrying colloids.

At the U.S. DOE's Hanford site in south-central Washington State, ^{137}Cs has leaked from underground waste tanks (*9*). The leaking tank waste consists of solutions of high alkalinity and ionic strength, main constituents of which are Na, OH, NO_3, NO_2, and Al (*10*). ^{137}Cs sorption to subsurface sediments is usually strong (*11*) but can be reduced under conditions of high ionic strength (*6, 12, 13*). The current depth distribution of ^{137}Cs below the SX tanks at Hanford can be explained by chromatographic tranport and ion exchange (*12, 14, 15*). As the contaminated plumes move downward through the vadose zone driven by gravity, the ionic strength of the plumes decreases due to dispersion and dilution with pore water (*16, 17*).

It has been demonstrated that colloids from the Hanford sediments can be mobilized when high ionic strength tank liquors are diluted by low ionic strength pore water (*18*). If such colloids contain Cs, either by sorption or coprecipitation, they also will facilitate the movement of Cs (*18*). Unknown, however, is the degree of colloid-facilitated transport. It has been suggested that, under natural subsurface conditions, colloid-facilitated radionuclide transport in general will not be very substantial because mobile colloidal concentrations in natural subsurface media are small (*19*). Moreover, under unsaturated conditions, laboratory column experiments have repeatedly shown that colloid transport is less pronounced than under saturated conditions (*20*−*25*).

The objective of this study was to quantitatively investigate transport of Cs through variably saturated Hanford sediments, as facilitated by colloids representative for Hanford leaking tank conditions. We hypothesize that Cs will desorb from Cs-carrying colloids as the colloids move through uncontaminated sediments, thereby counteracting the colloid-enhanced transport mechanism. We further hypothesize that the sediments' water saturation will affect Cs desorption from colloids, whereby less Cs desorbs from colloids as the water saturation decreases.

Materials and Methods

Artificial Pore Water. The artificial pore water (APW) for the column transport experiments consisted of 1.67 mM $NaHCO_3$ and 1.67 mM Na_2CO_3 (ionic strength $I = 6.67$ mM, pH 10). The artificial pore water was filtered with a 0.1 μm nylon membrane filter and degassed by helium bubbling. The APW offers a stable chemistry and prevents dissolution of carbonates present in the sediments. As APW is pH buffered, the degassing process has no or minimal impact on pH. This APW has a much lower ionic strength than the contaminant plumes below the Hanford waste tanks; however, the plumes become diluted with uncontaminated low ionic strength pore water and infiltrating meteoric water as the plumes move

* Corresponding author phone: (509)335-1719; fax: (509)335-8674; e-mail: flury@mail.wsu.edu.

10.1021/es048978+ CCC: $30.25
Published on Web 04/06/2005

TABLE 1. Selected Colloid and Sediment Characteristics

material	particle diameter[a] (nm)	electrophoretic mobility[a] (μm s^{-1})/(V cm^{-1})	surface area[b] (m^2/g)	mineralogy[c]
native colloids	393 ± 8	−3.5 ± 0.1	78.8 ± 0.3	chlorite, smectite, kaolinite, illite, quartz
modified colloids	407 ± 10	−3.6 ± 0.1	60.5 ± 0.8	cancrinite, sodalite, chlorite, smectite, illite, quartz
Hanford sediment	1.37 × 10^6	na[d]	3.63 ± 0.02	feldspar, mica, pyroxene, chlorite, smectite, illite, quartz

[a] Colloids: *Z*-averaged hydrodynamic diameter determined by dynamic light scattering in pH 10 $NaHCO_3/Na_2CO_3$ buffer solution (I = 6.67mM) (Zetasizer 3000HSA with a Helium−Neon laser of 633 nm wavelength, Malvern Instruments Ltd., Malvern, UK). Sediment: median diameter of weight-based particle size distribution. [b] Surface area measured with N_2 adsorption (ASAP 2010, Micromeritics Corporation, Norcross, GA). [c] Determined by X-ray diffraction with Cu Kα radiation (Philips XRG 3100, Philips Analytical Inc., Mahwah NJ) or petrographic thin sections. [d] na, not available

downward (*16*, *17*). At the low ionic strength of our APW colloid transport is favored; therefore, our experiments constitute a scenario where colloid-facilitated Cs transport is optimal at the Hanford site.

Porous Medium and Colloids. Sediments and colloids used in this study were similar to the ones used in a previous study (*25*). We briefly summarize the procedures here. Hanford sediments were sieved through a 2-mm sieve and extensively flushed with 1 M NaCl buffered at pH 10 with 1.67 mM $NaHCO_3$/1.67 mM Na_2CO_3 to saturate the exchange sites with Na, followed by a flush with APW. Particles with diameter <2 μm were fractionated from the sediments using gravity sedimentation to obtain a porous medium with particle size ranging from 2 to 2000 μm in diameter. The particles <2 μm were used as the colloidal source materials for the colloid-facilitated transport experiments.

The colloidal source materials were further fractionated by gravity settling for 2 weeks in APW. Suspended colloids were decanted and used for the transport experiments. We denote these colloids as "native colloids". To produce colloidal materials representative for a Hanford tank leak, Hanford sediments were reacted with a caustic solution (*26*). The colloidal materials were fractionated from the reacted sediments as described for the unreacted sediments. We denote those latter colloids as "modified" as opposed to "native". Both types of colloids were washed with deionized water to remove entrained salts. Selected colloidal characteristics are listed in Table 1. Particle diameters and electrophoretic mobility differ somewhat from the values reported in Cherrey et al. (*25*), and we attribute these differences to natural variability in the sedimental source material used.

While the packed columns do not represent the undisturbed sediments at Hanford, the pretreatment of the sediments was necessary to prevent in situ colloid mobilization. Consequently, our columns do not exactly mimic conditions at Hanford, but they allow us to conduct colloid transport experiments under well-controlled conditions.

Cesium. We used ^{137}Cs (specific activity 4.9 Ci/g or 1.81 × 10^{11} Bq/g; Isotope Products Laboratories, Valencia, CA) in the form of CsCl. Concentrations of ^{137}Cs were determined using a liquid scintillation analyzer (1900 TR, Packard Instrument Company, Meriden, CT) against external standards of ^{133}Ba (18.8 ± 0.2 mCi).

Cesium Sorption Isotherms. Batch sorption isotherms were used to determine the sorption of ^{137}Cs on colloids and sediments in the APW solution. A series of 250-mL Erlenmeyer flasks containing ^{137}Cs at concentrations ranging from 0 to 28.4 nM (687 Bq/mL) in 100 mL of native colloid suspension at a colloid concentration of about 10 mg/L were placed on a stir plate and mixed gently with a stir bar. ^{137}Cs concentrations ranging from 0 to 30.0 nM (726 Bq/mL) were used for modified colloids. For sediment sorption isotherms, 1.0 g of sediment and 100 mL of solution were used. Initial ^{137}Cs concentrations ranged from 0 to 68.8 nM (1665 Bq/mL). After 24 h, the suspensions were centrifuged at 16100*g* for 15 min. On the basis of Stokes' law, particles greater than 60 nm equivalent diameter should be centrifuged out. ^{137}Cs concentrations in the supernatant were measured, and the ^{137}Cs sorbed on colloids was calculated based on mass balance. All experiments were performed in triplicate.

Column Experiments. Column transport experiments were conducted using an acrylic column with 5.0 cm i.d. × 20.0 cm length. A detailed description and a schematic of the experimental apparatus are given elsewhere (*25*). Hanford sediments, which had particles less than 2 μm removed, were incrementally packed into the column and had a porosity of ≈0.4, a bulk density of 1.54 g/cm^3, and a pore volume of 152.3 cm^3. All experiments were conducted with one single column.

Colloids suspended in APW were fed into the column using a sprinkler head. The boundary condition at the bottom was controlled by a porous plate and a hanging water column. Column transport experiments were performed under steady-state flow conditions at effective water saturations varying from S_e = 0.2−1.0. Effective water saturation is defined as $S_e = (\theta - \theta_r)/(\theta_s - \theta_r)$, where θ is the volumetric water content, θ_s = 0.394 cm^3/cm^3 is the saturated water content, and θ_r = 0.074 cm^3/cm^3 is the residual water content. Volumetric water contents and matric potentials were maintained steady and uniform for each run by balancing the inflow rate and the hanging water column.

Colloid suspensions (≈10 mg/L) were equilibrated with known amounts of ^{137}Cs for 24 h before being introduced into the column. From the Cs sorption isotherm experiments, equilibrium was found to be reached within at least 24 h. Outflow colloid concentrations were measured using an in-line spectrophotometer (LC95 UV/VIS, Perkin-Elmer, Norwalk, CT) at a wavelength of 300 nm. Outflow suspensions were collected using a fraction collector and divided into two aliquots. One of these aliquots was measured for ^{137}Cs directly using the liquid scintillation analyzer, and the other aliquot was centrifuged at 16100*g* for 15 min. The supernatant was measured for ^{137}Cs. The first aliquot yields total ^{137}Cs concentrations, the second aliquot yields dissolved ^{137}Cs concentrations, and Cs concentrations on the colloids were calculated by mass balance.

Under water-saturated conditions, we conducted a series of experiments with different Cs loadings on the colloids at the same pore water velocity (10 cm/min). We used ^{137}Cs at concentrations of 5.63 nM (136 Bq/mL), 10.1 nM (244 Bq/mL), 16.1 nM (390 Bq/mL) and 28.4 nM (687 Bq/mL) preequilibrated with native colloids for 24 h as the injectant. ^{137}Cs at concentrations of 7.59 nM (184 Bq/mL), 12.6 nM (305 Bq/mL), 23.8 nM (576 Bq/mL), and 30.0 nM (726 Bq/mL) were used for modified colloids. To investigate the effect of pore water velocity on Cs transport, native colloids preequilibrated with 27.4 nM (663 Bq/mL) and modified colloids preequilibrated with 32.5 nM (786 Bq/mL) were introduced into the column at pore water velocities of ≈1 cm/min to 10 cm/min. To check whether the retained Cs within the column from previous runs may interfere with the results of the following Cs breakthrough experiments,

we repeated some of the Cs transport experiments after completion of the full sequence of water-saturated breakthrough experiments.

Under water-unsaturated conditions, the Cs loading on the colloids was kept constant, but we varied the effective water saturation S_e in increments of 0.1 by decreasing effective water content from 1.0 to 0.2. We used ^{137}Cs at a concentration of 8.76 nM (212 Bq/mL) preequilibrated with both native and modified colloids for 24 h as the injectant. Each set of colloid breakthroughs was preceded by a nitrate (0.2 mM $NaNO_3$) breakthrough experiment to determine the hydrodynamics of the column. Nitrate was measured with the spectrophotometer at 204 nm wavelength. All experiments were conducted at 20−22 °C.

Modeling of Colloid Breakthrough Curves. We describe colloid transport through the Hanford sediment columns with the two-region transport model (*27*). From our previous (*25*) and current experimental observations, we have evidence that there is no colloid deposition at the liquid−solid interface. We believe that retained colloids in the column are either captured at the liquid−gas interface by film-straining (*21*, *23*) or captured at the solid−liquid−gas three-phase interface due to physical constraint (*21*, *28*). These colloid-capturing actions most likely occur from the mobile region. Thus, we assume that colloids are only deposited within the mobile region only:

$$\frac{\partial(\theta_m c_m)}{\partial t} + \frac{\partial(\theta_{im} c_{im})}{\partial t} = \frac{\partial}{\partial z}\left(\theta_m D_m \frac{\partial c_m}{\partial z}\right) - \frac{\partial(q_m c_m)}{\partial z} - \theta_m \lambda_m c_m \quad (1)$$

$$\frac{\partial(\theta_{im} c_{im})}{\partial t} = \alpha(c_m - c_{im}) \quad (2)$$

where c_m and c_{im} refer to the colloid concentrations in the mobile and immobile phases, respectively; θ_m and θ_{im} refer to the mobile and immobile water, respectively; q_m denotes the Darcy velocity of the mobile water; λ_m is the colloid deposition coefficient from the mobile water phase; D_m is the colloid dispersion coefficient in the mobile phase; and α is the colloid transfer coefficient between mobile and immobile water. Taking the water content constant and using dimensionless variables, we can write eqs 1 and 2 as

$$\beta\frac{\partial C_m}{\partial T} + (1-\beta)\frac{\partial C_{im}}{\partial T} = \frac{1}{Pe}\frac{\partial^2 C_m}{\partial Z^2} - \frac{\partial C_m}{\partial Z} - \mu_m C_m \quad (3)$$

$$(1-\beta)\frac{\partial C_{im}}{\partial T} = \omega(C_m - C_{im}) \quad (4)$$

where C denotes dimensionless colloid concentrations ($C_m = c_m/c_0$ and $C_{im} = c_{im}/c_0$) with c_0 being the colloid concentration in the inflow. The dimensionless time is defined as $T = vt/L$, and the space is defined as $Z = z/L$, where L is the length of the column. The dimensionless parameters are defined as

$$\beta = \frac{\theta_m}{\theta} \quad \text{(fraction of mobile water)} \quad (5)$$

$$Pe = \frac{vL}{\beta D_m} \quad \text{(Peclet number)} \quad (6)$$

$$w = \frac{\alpha L}{\theta v} \quad \text{(mass transfer coefficient)} \quad (7)$$

$$\mu_m = \frac{\beta\lambda_m L}{v} = \frac{\lambda_m L}{v_m} \quad \text{(deposition coefficient)} \quad (8)$$

where $v = q_m/\theta$ is the pore water velocity, $\theta = \theta_m + \theta_{im}$, and $v_m = v/\beta$. An analytical solution of eqs 3 and 4 with Dirichlet boundary conditions was fitted to experimental colloid breakthrough curves using CXTFIT (*29*).

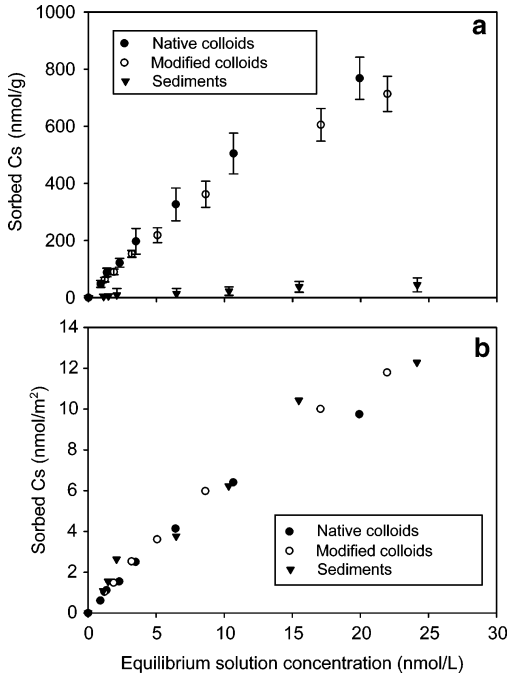

FIGURE 1. Cs sorption isotherms for Hanford native and modified colloids and Hanford sediments. Symbols are averaged sorbed Cs concentrations with respect to aqueous concentrations. Error bars denote ± one standard error. Sorbed Cs concentrations are expressed in terms of mass (a) and surface area (b).

Results and Discussion

Cesium Sorption on Colloids and Sediments. Native colloids had a higher sorption affinity for Cs than the modified colloids, although the differences were not pronounced (Figure 1a). The Cs sorption affinity to the Hanford sediments was considerably less than for the colloids. We related the amount of Cs sorbed on the solids (nmol/g) to the amount of Cs sorbed per surface area of the solids (nmol/m^2) by dividing the former by the specific surface area of the solids shown in Table 1. Cs sorption is an ion exchange reaction that is related to particle surface area. When the Cs sorption was normalized by the surface area of the solids, the sorption isotherms were superimposed (Figure 1b). This indicates that the sorption affinity of Cs to colloids and sediment surfaces was similar. Colloids were derived from the sediments, and apparently the sorption expressed in terms of surface area was similar between colloids and sediments. Such a case was denoted by Honeyman and Ranville (*19*) as a symmetrical system.

Column Water Contents and Water Potentials. Steady-state flow experiments, with uniform unit-gradient conditions, were attempted at effective saturations $S_e = 0.1, ..., 1.0$ in 0.1 increments. However, $S_e = 0.9$ was not possible due to flow restrictions in the porous plate and outflow tubing, and $S_e = 0.1$ was not possible because no stable background colloid concentration after colloid breakthrough could be obtained. The remaining saturations were achieved with steady-state and uniform unit-gradient conditions for most of the column, except for the top and bottom 2.5 cm. The top of the column was dryer (more negative matric potential readings), and the bottom of the column was wetter (less negative matric potential readings) than the middle. The results were similar to the ones reported by Cherrey et al. (*25*), to which we refer for details on tensiometer and water content readings.

TABLE 2. Hanford Native and Modified Colloid Transport Parameters Using the Two-Region Transport Model[a]

measured parameters			fitted parameters[b]					
effective water saturation (−)	gravimetric water content (kg/kg)	v^c (cm/min)	v^d (cm/min)	D (cm²/min)	β (−)	ω (−)	μ_m (−)	R^2 (−)
				Native Colloids				
1.0	0.25	10.03	12.89	26 ± 3				0.9940
0.80	0.23	9.50	10.32	17 ± 2			0.21 ± 0.01	0.9927
0.70	0.21	7.71	6.99	23 ± 6	0.86 ± 0.10	0.25 ± 0.23	0.26 ± 0.01	0.9950
0.60	0.19	7.00	6.10	26 ± 5	0.79 ± 0.08	0.68 ± 0.45	0.21 ± 0.01	0.9953
0.50	0.17	6.85	5.93	17 ± 3	0.41 ± 0.06	2.20 ± 0.51	0.33 ± 0.01	0.9952
0.40	0.15	6.62	5.34	25 ± 2	0.74 ± 0.05	0.76 ± 0.27	0.46 ± 0.01	0.9966
0.30	0.12	6.17	5.30	9 ± 1	0.50 ± 0.01	1.07 ± 0.04	0.65 ± 0.01	0.9993
0.20	0.08	6.13	5.10	6 ± 1	0.44 ± 0.01	1.0 ± 0.05	0.98 ± 0.01	0.9979
				Modified Colloids				
1.0	0.25	10.10	12.89	32 ± 4				0.9893
0.80	0.23	9.94	10.32	12 ± 1			0.02 ± 0.01	0.9968
0.70	0.21	8.25	6.99	16 ± 1	0.81 ± 0.01	0.03 ± 0.01	0.06 ± 0.01	0.9987
0.60	0.19	6.58	6.10	14 ± 2	0.79 ± 0.03	0.29 ± 0.06	0.16 ± 0.01	0.9991
0.50	0.17	5.65	5.93	21 ± 2	0.38 ± 0.04	1.71 ± 0.17	0.23 ± 0.01	0.9956
0.40	0.15	5.12	5.34	35 ± 1	0.41 ± 0.03	1.42 ± 0.10	0.40 ± 0.01	0.9972
0.30	0.12	5.00	5.30	nf	nf	nf	nf	nf
0.20	0.08	4.87	5.10	nf	nf	nf	nf	nf

[a] v, pore water velocity; D, hydrodynamic dispersion; β, fraction of mobile water; ω, mass transfer coefficient; μ_m, rate coefficient for colloid deposition; R^2, coefficient of determination; nf, fit not possible due to high parameter correlations. [b] Values are fitted parameters ± one standard error. [c] Calculated from measured water flux J_w and effective water saturation S_e as $v = J_w/(S_e\theta_s)$. [d] Fitted from nitrate breakthrough curves.

Nitrate and Colloid Transport. The nitrate and colloid data could be well-described with the two-region model, and the results suggest a significant fraction of immobile water when the effective water saturation dropped below 0.8 (Table 2). Under water saturated conditions, both native and modified colloids were quantitatively recovered, and no colloids were deposited inside the column. When the column became unsaturated, colloids began to be retained in the sediment. At an effective water saturation of 0.2, ≈60% of colloids was retained within the column. These colloids were mostly likely retained near the liquid−gas−solid three-phase interface (*30*).

Colloid mass transfer coefficients (ω) did not show a trend as function of water saturation, and the estimated values were associated with large errors (Table 2). Colloid deposition coefficients (μ_m) increased with decreasing system saturation. Both the dimensionless and the dimensional deposition coefficients (μ_m and λ_m, respectively) showed a pronounced dependence on water saturation (Figure 2). The fraction of mobile water (β) decreases with decreasing water saturation (Table 2).

Colloid-Facilitated Cesium Transport under Saturated Conditions. Dissolved Cs could not breakthrough Hanford sediments at either a concentration of 7.66 nM (185 Bq/mL) or 30.6 nM (760 Bq/mL) for a 3 pore volume pulse injectant. In our experiments, where the total time allowed to develop the breakthrough curves was about 8 pore volume, Cs breakthrough only occurred in the presence of colloids. We therefore conclude that cesium could move substantial distances only when associated with colloids. Also, from our previous research, we have evidence that Cs cannot breakthrough the column in the presence of 1 mM NaCl until 950 pore volume have passed (*18*). However, Cs concentrations on the colloids in the effluent were smaller than in the influent, indicating that Cs desorbed from the colloids during the transport through the column.

Cs breakthrough curves, with the same pore velocity, expressed in relation to the total Cs concentration in the inflow are illustrated in Figure 3a. The ratio on the y-axis is defined as $C_{Cs}C_{colloid}/C_{0T}$, where C_{0T} is the sum of sorbed and solution-phase Cs concentration in the inflow; C_{Cs} is the Cs concentration on the colloids in the outflow; and $C_{colloid}$ is the colloid concentration in the outflow. This ratio is the amount of Cs sorbed on colloids in the outflow divided by the total amount of Cs (sorbed and in solution) in the inflow. Figure 3a indicates that the higher the input Cs concentration, the lower the $C_{Cs}C_{colloid}/C_{0T}$ value. This phenomenon, which was more pronounced for native than modified colloids, was likely caused by the nonlinearity of the Cs sorption isotherms. Under water-saturated conditions, only about 8−16% of the total Cs infused in the column could be recovered in the outflow (Table 3).

It is possible that the retained Cs within the column from previous runs may interfere with the results of the following

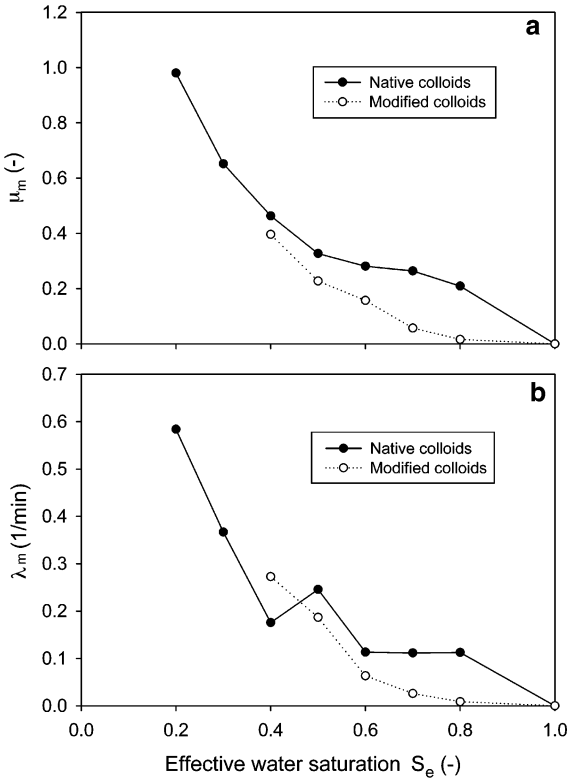

FIGURE 2. Colloid deposition coefficients μ_m (a) and λ_m (b) as function of water saturation.

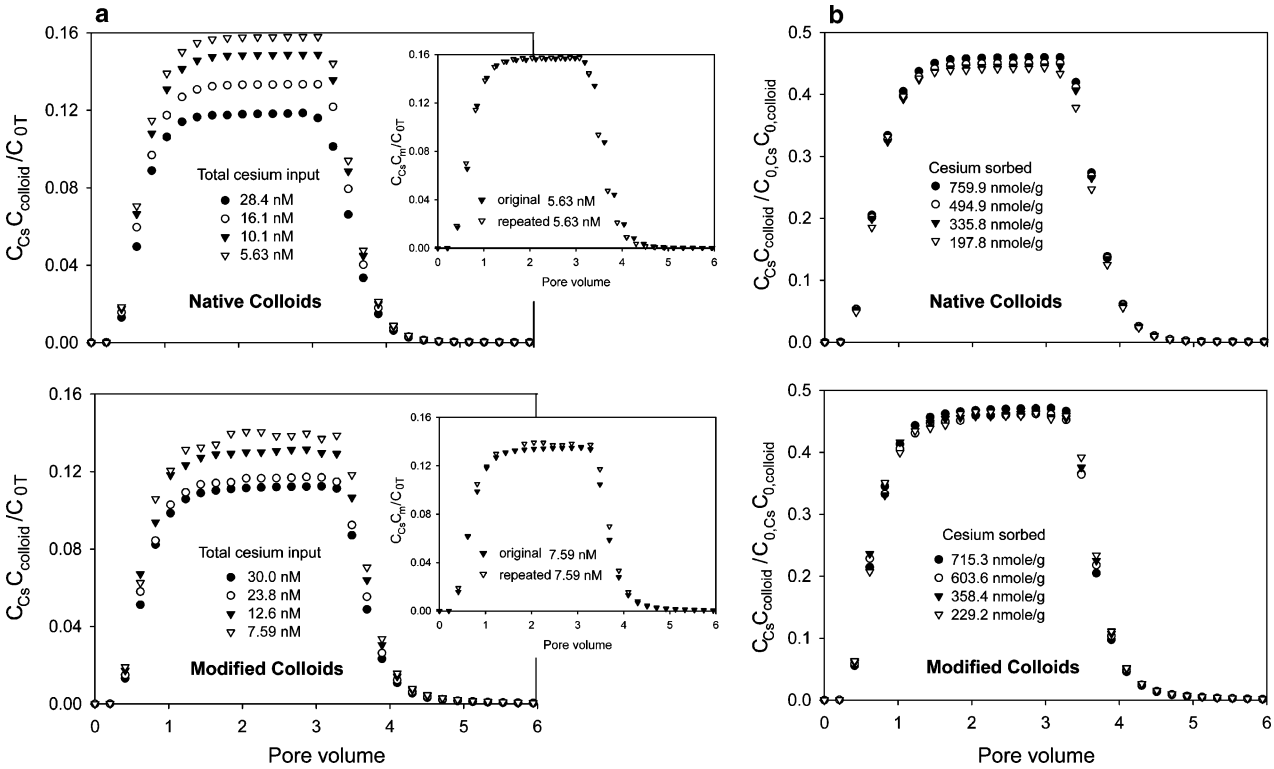

FIGURE 3. Cesium breakthrough data (a) with regard to total amount of Cs in inflow and (b) with regard to initially sorbed Cs on colloids under water-saturated flow conditions. Insets show comparison between Cs breakthrough curves at the beginning and at the end of the experimental sequence.

TABLE 3. Colloid and Cesium Mass Recovery in Column Outflow

		colloid recovery		Cs loading on colloids[a]		Cs mass recovery[b]		Cs stripped off colloids[c]	
effective water saturation (−)	pore water velocity (native/modified) (cm/min)	native colloids (%)	modified colloids (%)	native colloids (nmol/g)	modified colloids (nmol/g)	native colloids (%)	modified colloids (%)	native colloids (%)	modified colloids (%)
				Saturated Flow Experiments					
1.0	10.0/10.1	96.3	100.5	760	715	11.8	11.3	58.6	52.7
1.0	10.0/10.1	93.7	98.4	495	604	13.4	11.8	58.1	50.7
1.0	10.0/10.1	93.3	98.1	336	358	14.9	13.4	56.9	51.0
1.0	10.0/10.1	97.9	100.6	198	230	15.9	14.2	55.6	50.4
1.0	10.5/10.4	99.4	97.4	763	726	11.5	9.64	54.4	53.9
1.0	8.21/7.87	98.7	98.6	790	751	10.1	8.45	62.4	62.2
1.0	6.62/5.47	97.8	99.5	808	771	8.38	8.01	70.1	66.5
1.0	5.41/4.61	100.6	102.1	823	790	8.82	8.05	70.6	67.1
1.0	1.01/0.94	98.6	101.9	780	741	9.29	8.28	72.4	70.0
				Unsaturated Flow Experiments					
0.8	9.50/9.94	83.9	98.7	429	364	24.6	29.6	40.0	27.6
0.7	7.71/8.25	77.9	93.6	432	389	22.9	28.1	40.5	32.2
0.6	7.0/6.58	77.0	87.2	446	417	22.5	26.4	42.4	36.5
0.5	6.85/5.65	73.4	81.4	457	429	21.5	24.6	43.7	38.3
0.4	6.63/5.13	65.5	69.4	474	436	19.3	20.9	45.6	39.4
0.3	6.17/5.0	54.3	59.5	488	452	15.9	17.9	47.3	41.5
0.2	6.13/4.88	40.1	44.9	497	467	11.8	13.5	48.2	43.4

[a] Cs concentration on colloids in column inflow. [b] Total amount of Cs recovered in outflow related to the total amount of Cs in inflow. [c] Amount of Cs on colloids in outflow related to the amount of Cs on colloids in inflow.

Cs breakthrough experiments. Due to the low Cs concentrations, however, the interference should be small. To test for possible interferences, we repeated some of the Cs transport experiments after completion of the full sequence of breakthrough experiments. Representative Cs breakthrough curves of these repetitions are shown in the insets of Figure 3. The Cs breakthrough curves were reproducible, precluding the possible history effect.

Figure 3b shows the Cs breakthrough curves at the same pore velocity but with different Cs loadings expressed in relation to the Cs concentration on the colloids. This ratio on the y-axis is defined as $C_{Cs}C_{colloid}/(C_{0,Cs}C_{0,colloid})$, where $C_{0,Cs}$ and C_{Cs} are the Cs concentrations on the colloids (nmol/g) in inflow and outflow, respectively, and $C_{0,colloid}$ and $C_{colloid}$ are the colloid concentrations (mg/L) in inflow and outflow, respectively. This ratio is the amount of Cs sorbed on colloids in the outflow divided by the amount of Cs sorbed on colloids in the inflow. When related to the colloid-sorbed Cs concentration in the inflow (Figure 3b), a constant fraction of Cs desorbed from the colloids, irrespective of the amount

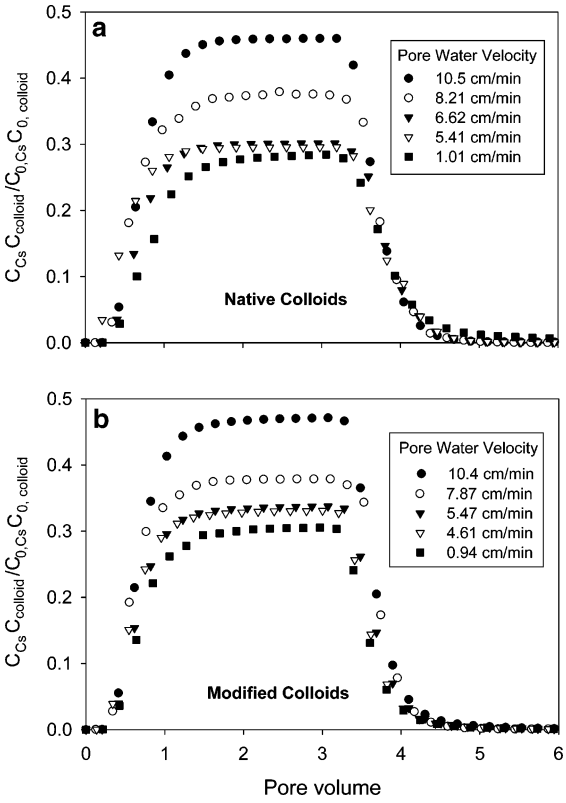

FIGURE 4. Cesium breakthrough data at different pore water velocities under water-saturated flow conditions. Symbols are experimental data. Cs concentrations are expressed relative to Cs sorbed on colloids in the inflow.

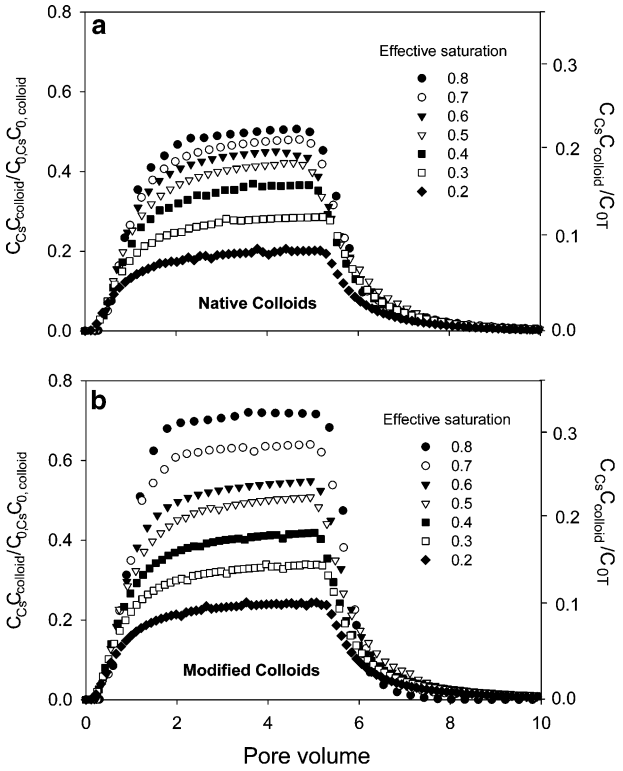

FIGURE 5. Cesium breakthrough data under unsaturated conditions. Cesium concentrations are related to initially sorbed Cs on colloids ($C_{Cs}C_{colloid}/C_{0,Cs}C_{0,colloid}$) and total amount of Cs in inflow ($C_{Cs}C_{colloid}/C_{0T}$).

of Cs initially sorbed on the colloids. The figure also shows that more than 50% of the Cs initially sorbed on the colloids was stripped off the colloids during transport. The greater the amount of initially colloid-sorbed Cs, the greater the absolute amount of Cs desorbed from the colloids during transport.

Colloid-facilitated cesium transport was impeded with decreasing pore velocity (Figure 4), suggesting that Cs desorption from colloids was, in part, a residence-time-dependent process. The Cs desorption from colloids was apparenty not a "pure" ion exchange equilibrium process. As the flow rate decreased, more Cs desorbed from colloids during transport. At the smallest pore water velocity (≈1 cm/min), 70−72% of the initially sorbed Cs was desorbed from the colloids during transport through the column.

Colloid-Facilitated Cs Transport under Unsaturated Conditions. Only a single Cs loading was used for the unsaturated colloid-facilitated Cs transport experiments. Consequently, Cs breakthrough curves expressed relative to colloidal Cs concentrations and relative to total Cs concentrations have the same shape and can be plotted in one graph with different concentration axes (Figure 5). As the water content of the porous medium decreased, colloid transport became less effective, and the fraction of Cs desorbed from the colloids increased (Table 3). This was likely due to the decrease of the water velocity with decreasing water saturation, which allows more time for Cs to desorb from colloids. As was the case under saturated flow conditions, less Cs was stripped off modified colloids than native colloids (Table 3). We attribute this to the different mineralogy of the colloids (i.e., the presence of the feldspathoids cancrinite and sodalite in the modified colloids). The feldspathoids cancrinite and sodalite contain cages and channels in which Cs can sorb (*31*). We believe that desorption from these cages and channels is diffusion-controlled and as such dependent on the residence time of the colloids inside the column.

Compared with water-saturated conditions, less Cs desorbed from colloids under unsaturated conditions. The percentage of Cs desorbed from the colloids under unsaturated conditions increased slightly with decreasing water content for native colloids but moderately for modified colloids (Table 3). Under unsaturated flow, a considerable amount of colloids was retained inside the column, and as we ran the unsaturated experiments in sequence of decreasing water contents, we expect that retained colloids will not be released in subsequent runs. The mass balance calculations shown in Table 3 are based on the amounts of Cs in the inflow and outflow and are therefore likely not biased by release of deposited colloids.

Assuming an equilibrium sorption process, we can calculate the ratio of Cs sorbed to colloids with respect to total Cs within the system. This ratio is given as (*19*)

$$\kappa = \frac{\text{amount of Cs on colloids}}{\text{total amount of Cs}} = \frac{q_{\text{colloid}} C_{\text{colloid}} S_{\text{e}}}{C_{\text{Cs}} S_e + q_{\text{colloid}} C_{\text{colloid}} S_{\text{e}} + q_{\text{sediment}} \rho_{\text{b}}/\epsilon} \quad (9)$$

where C_{Cs} and C_{colloid} are the solution-phase Cs and colloid concentrations, respectively; q is the sorbed-phase Cs concentration on colloids or sediments; ρ_{b} is the bulk density; and ϵ is the porosity. The three terms in the denominator of eq 9 represent, respectively, the solution-phase, the colloid-phase, and the sediment-phase Cs concentrations. On the basis of the sorption isotherms, we calculated the Cs concentrations associated with the different phases. Solution- and colloid-phase Cs concentrations were 4 orders of magnitude smaller than the sediment-phase concentrations,

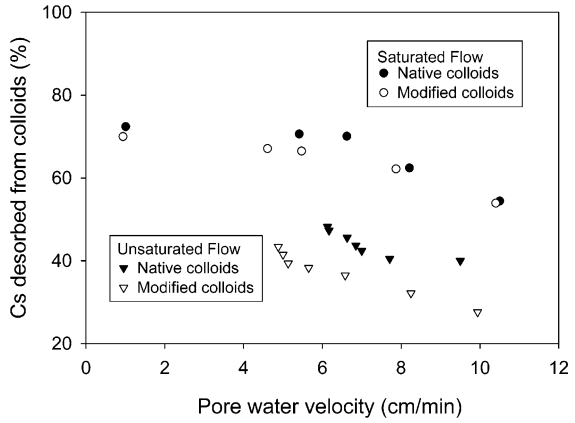

FIGURE 6. Cesium desorbed from colloids during transport through sediment column as a function of the measured pore water velocity $v = q_m/\theta$.

and we can therefore simplify eq 9 to

$$\kappa = \frac{q_{\text{colloid}} C_{\text{colloid}} S_e}{q_{\text{sediment}} \rho_b / \epsilon} = \frac{K_{\text{colloid}} A_{\text{colloid}} C_{\text{colloid}} S_e}{K_{\text{sediment}} A_{\text{sediment}} \rho_b / \epsilon} \quad (10)$$

where K denotes the sorption coefficient (mL/m^2) for colloids or sediments, and A denotes the specific surface area (m^2/g) for colloids and sediments. For a symmetrical system (*19*) as in our case, $K_{\text{colloid}} = K_{\text{sediment}}$, and eq 10 reduces to

$$\kappa = \frac{A_{\text{colloid}} C_{\text{colloid}} S_e}{A_{\text{sediment}} \rho_b / \epsilon} \quad (11)$$

On the basis of eq 11, only a small fraction of Cs would associate with the colloids: the fraction κ ranges from $\kappa = 1 \times 10^{-5}$ at effective saturation of $S_e = 0.2$ to $\kappa = 5 \times 10^{-5}$ at effective saturation of $S_e = 1.0$. On the contrary, our experimental Cs breakthrough curves show that a much larger fraction of Cs was transported by colloids than what would be expected based on the equilibrium sorption assumption. Our data suggest that a portion of the Cs sorbed to colloids could not readily be desorbed and contributed to the increased degree of colloid-facilitated Cs transport.

There was a general trend that less Cs desorbed from colloids during transport as water flow rates increased (Figure 6), likely because of the smaller residence times at higher flow rates. However, under similar flow rates, less Cs desorbed from colloids during unsaturated flow than during saturated flow. We think that during unsaturated flow, less Cs sorption sites on the sediments are available to strip off the Cs from colloids because less sediment surface area is in contact with the mobile flow regions. Furthermore, as the water content decreased, the immobile water fraction increased, indicating that colloids moved through a smaller effective cross-section of the porous medium. That would further decrease the amount of sediment sorption sites available to strip Cs from the colloids.

Implications for Colloid-Facilitated Cs Transport at the Hanford Site. At the Hanford site, an important question is whether Cs that has leaked into the vadose zone can reach the underlying groundwater. From core sampling in the S-SX tank farm, we know that peak concentrations of ^{137}Cs are located at 25−26 m depth below ground, with traces of ^{137}Cs found up to 38 m below ground (*16*, *32*). Based on the results of our laboratory study, it is unlikely that colloids were responsible for the movement of the Cs to these depths. If Cs is reversibly attached to to colloids by ion exchange, Cs would likely be stripped off the colloids as the colloids move through uncontaminated sediments. The sediments underlying Hanford waste tanks sorb Cs with high affinity (*12*, *33*), and this would provide an effective means of opposing colloid-facilitated Cs transport. Other studies have indeed shown that the current location of Cs under Hanford SX waste tanks can be explained by chromatographic solution-phase transport in a high electrolyte waste solution (*14*, *15*, *17*).

In addition, colloid transport itself is restricted in the vadose zone, and with decreasing moisture content, the restriction becomes more obvious. In this study, we show that ≈55−60% of initially present colloids are retained in the column at an effective water saturation of 0.2. At the Hanford site, gravimetric water saturations in sediments of the Hanford formation underlying the S-SX waste tanks range from 0.04 to 0.17 kg/kg (*16*), and the thickness of the vadose zone varies from 40 to 100 m (*33*, *34*). We conducted our column experiments with gravimetric water contents in the ranged of 0.08−0.25 kg/kg (Table 2) and in a column of 20 cm length. The possibility of colloids to be transported from the soil surface to the groundwater at the Hanford tank farms appears minimal, unless water contents and flow rates are locally and temporally increased by snowmelt events or artifical infiltration caused by past waste management practices.

Acknowledgments

This research was supported by the Office of Science (BER), U.S. Department of Energy, Grant DE-FG07-05ER62882. We thank John Zachara and Jeff Serne (Pacific Northwest National Laboratory) for providing us with the Hanford sediments, Hongting Zhao for synthesis of the modified colloids, and Jeff Smith (USDA-ARS Pullman) for allowing us to use his liquid scintillation analyzer.

Literature Cited

(1) Ryan, J. N.; Illangasekare, T. H.; Litaor, M. I.; Shannon, R. Particle and plutonium mobilization in macroporous soils during rainfall simulations. *Environ. Sci. Technol.* **1998**, *32*, 476−482.
(2) Kersting, A. B.; Efurd, D. W.; Finnegan, D. L.; Rokop, D. J.; Smith, D. K.; Thompson, J. L. Migration of plutonium in ground water at the Nevada Test Site. *Nature* **1999**, *397*, 56−59.
(3) Grolimund, D.; Borkovec, M.; Barmettler, K.; Sticher, H. Colloid-facilitated transport of strongly sorbing contaminants in natural porous media: a laboratory column study. *Environ. Sci. Technol.* **1996**, *30*, 3118−3123.
(4) Saiers, J. E.; Hornberger, G. M. The role of colloidal kaolinite in the transport of cesium through laboratory sand columns. *Water Resour. Res.* **1996**, *32*, 33−41.
(5) Noell, A. L.; Thompson, J. L.; Corapcioglu, M. Y.; Triay, I. R. The role of silica colloids on facilitated cesium transport through glass bead columns and modeling. *J. Contam. Hydrol.* **1998**, *31*, 23−56.
(6) Saiers, J. E.; Hornberger, G. M. The influence of ionic strength on the facilitated transport of cesium by kaolinite colloids. *Water Resour. Res.* **1999**, *35*, 1713−1727.
(7) Zhuang, J.; Flury, M.; Jin, Y. Colloid-facilitated Cs transport through water-saturated Hanford sediment and Ottawa sand. *Environ. Sci. Technol.* **2003**, *37*, 4905−4911.
(8) Aharoni, C.; Pasricha, N. S.; Sparks, D. L. Adsorption and desorption kinetics of cesium in an organic matter rich soil saturated with different cations. *Soil Sci.* **1992**, *156*, 233−239.
(9) Gephart, R. E.; Lundgren, R. E. *Hanford Tank Cleanup: A Guide to Understanding the Technical Issues*, 4th ed.; Battelle Press: Columbus, OH, 1998.
(10) Serne, R. J.; Zachara, J. M.; Burke, D. S. *Chemical Information on Tank Supernatants, Cs Adsorption from Tank Liquids onto Hanford Sediments, and Field Observations of Cs Migration from Past Tank Leaks*; Pacific Northwest National Laboratory,: Richland, WA, 1998; PNNL-11495/UC-510.
(11) Cornell, R. M. Adsorption of cesium on minerals: a review. *J. Radioanal. Nucl. Chem.* **1993**, *171*, 483−500.
(12) Zachara, J. M.; Smith, S. C.; Liu, C.; McKinley, J. P.; Serne, R. J.; Gassman, P. L. Sorption of Cs^+ to micaceous subsurface sediments from the Hanford Site, USA. *Geochim. Cosmochim. Acta* **2002**, *66*, 193-211.
(13) Flury, M.; Czigany, S.; Chen, G.; Harsh, J. B. Cesium migration in saturated silica sand and Hanford sediments as impacted by ionic strength. *J. Contam. Hydrol.* **2004**, *71*, 111−126.

(14) Knepp, A. J. *Field Investigation Report for Waste Management Area S-SX*; RPP-7884, Rev. 0, CH2M HILL Hanford Group, Inc.: Richland, WA, 2002.
(15) Steefel, C. I.; Carroll, S.; Zhao, P.; Roberts, S. Cesium migration in Hanford sediment: a multisite cation exchange model based on laboratory transport experiments. *J. Contam. Hydrol.* **2003**, *67*, 219−246.
(16) Serne, R. J.; Clayton, R. E.; Kutnyakov, I. V.; Last, G. V.; LeGore, V. L.; Wilson, T. C.; Schaef, H. T.; O'Hara, M. J.; Wagnon, K. B.; Lanigan, D. C.; Brown, C. F.; Williams, B. A.; Lindenmeier, C. W.; Orr, R. D.; Burke, D. S.; Ainsworth, C. C. *Characterization of Vadose Zone Sediment: Borehole 41-09-39 in the S-SX Waste Management Area*; Pacific Northwest National Laboratory, U.S. Department of Energy: Richland, WA, 2002; PNNL-13757-3.
(17) Lichtner, P. C.; Yabusaki, S.; Pruess, K.; Steefel, C. I. Role of competitive cation exchange on chromatographic displacement of cesium in the vadose zone beneath the Hanford S/SX tank farm. *Vadose Zone J.* **2004**, *3*, 203−219.
(18) Flury, M.; Mathison, J. B.; Harsh, J. B. In situ mobilization of colloids and transport of cesium in Hanford sediments. *Environ. Sci. Technol.* **2002**, *36*, 5335−5341.
(19) Honeyman, B. D.; Ranville, J. F. Colloid properties and their effects on radionuclide transport through soils and groundwater. In *Geochemistry of Soil Radionuclides*; Zhang, P.-C., Brady, P. V., Eds.; SSSA Special Publication 59; Soil Science Society of America: Madison, WI, 2002; pp 131−163.
(20) Wan, J. M.; Wilson, J. L. Colloid transport in unsaturated porous media. *Water Resour. Res.* **1994**, *30*, 857−864.
(21) Wan, J. M.; Tokunaga, T. K. Film straining of colloids in unsaturated porous media: conceptual model and experimental testing. *Environ. Sci. Technol.* **1997**, *31*, 2413−2420.
(22) Schäfer, A.; Ustohal, P.; Harms, H.; Stauffer, F.; Dracos, T.; Zehnder, A. J. B. Transport of bacteria in unsaturated porous media. *J. Contam. Hydrol.* **1998**, *33*, 149−169.
(23) Lenhart, J. J.; Saiers, J. E. Transport of silica colloids through unsaturated porous media: experimental results and model comparisons. *Environ. Sci. Technol.* **2002**, *36*, 769−777.
(24) Jewett, D. G.; Logan, B. E.; Arnold, R. G.; Bales, R. C. Transport of *Pseudomonas fluorescences* strain P17 through quartz sand columns as a function of water content. *J. Contam. Hydrol.* **1999**, *36*, 73−89.
(25) Cherrey, K. D.; Flury, M.; Harsh, J. B. Nitrate and colloid transport through coarse Hanford sediments under steady state, variably saturated flow. *Water Resour. Res.* **2003**, *39*, 1165, doi: 10.1029/2002WR001944.
(26) Mashal, K.; Harsh, J. B.; Flury, M.; Felmy, A. R.; Zhao, H. Colloid formation in Hanford sediments reacted with simulated tank waste. *Environ. Sci. Technol.* **2004**, *38*, 5750−5756.
(27) van Genuchten, M. T.; Wagenet, R. J. Two-site/two-region models for pesticide transport and degradation: theoretical development and analytical solutions. *Soil Sci. Soc. Am. J.* **1989**, *53*, 1303−1310.
(28) Crist, J. T.; McCarthy, J. F.; Zevi, Y.; Baveye, P. C.; Troop, J. A.; Steenhuis, T. S. Pore-scale visualization of colloid transport and retention in partially saturated porous media. *Vadose Zone J.* **2004**, *3*, 444−450.
(29) Toride, N.; Leij, F. J.; van Genuchten, M. T. *The CXTFIT Code for Estimating Transport Parameters from Laboratory or Field Experiments*, Version 2.1; Research Report 137; U.S. Salinity Laboratory: Riverside, CA, 1995.
(30) Chen, G.; Flury, M. Retention of mineral colloids in unsaturated porous media as related to their surface properties. *Colloids Surf. Physicochem. Eng. Aspects* **2005**, *256*, 207−216.
(31) Zhao, H.; Deng, Y.; Harsh, J. B.; Flury, M.; Boyle, J. S. Alteration of kaolinite to cancrinite and sodalite by simulated Hanford tank wastes and its impact on cesium retention. *Clays Clay Miner.* **2004**, *52*, 1−13.
(32) Serne, R. J.; Clayton, R. E.; Kutnyakov, I. V.; Last, G. V.; LeGore, V. L.; Wilson, T. C.; Schaef, H. T.; O'Hara, M. J.; Wagnon, K. B.; Lanigan, D. C.; Brown, C. F.; Williams, B. A.; Lindenmeier, C. W.; Orr, R. D.; Burke, D. S.; Ainsworth, C. C. *Characterization of Vadose Zone Sediment: Slant Borehole SX-108 in the S-SX Waste Management Area*; Pacific Northwest National Laboratory, U.S. Department of Energy: Richland, WA, 2002; PNNL-13757-4.
(33) McKinley, J. P.; Zeissler, C. J.; Zachara, J. M.; Serne, R. J.; Lindstrom, R. M.; Schaef, H. T.; Orr, R. D. Distribution and retention of Cs-137 in sediments at the Hanford site, Washington. *Environ. Sci. Technol.* **2001**, *35*, 3433−3441.
(34) Gee, G. W.; Heller, P. R. *Unsaturated Water Flow at the Hanford Site: A Review of Literature and Annotated Bibliography*; Pacific Northwest National Laboratory: Richland, WA, 1985.

Received for review July 3, 2004. Revised manuscript received March 4, 2005. Accepted March 7, 2005.

ES048978+